Relationship between high-frequency tremor and a large earthquake

Fumitaka Inuyama · Kyushu Electric Power Co. Inc.(retired) Senior power engineer

In earthquakes, after strong stress accumulates on a wide fault plane with a vast number of asperities, most asperities collapse in an avalanche manner. During the energy accumulation of growth processes leading to large earthquakes, some fragile asperities cannot withstand the increasing stress and collapse before major earthquakes. The impact force of the collapse of the fragile asperity causes the bedrock to tremble. At this time, the bedrock is still in the process of energy accumulation, and significant stress is at work, so the vibrations can sometimes become high-frequency modes.To illustrate this mathematically, the seismic plate is modeled as an elastic strip beam, and the bending vibration equation in which the beam experiences damping c and stress s is given by Equation 1. It solves the partial differential equation using the variable separation method $\boldsymbol{y(x,t) = X(x) \cdot T(t)}$. as bilateral simple supports. (density ρ, length L, area A, Young modulus E, second moment I)

$$\rho A\frac{\partial^2 y}{\partial t^2} + c\frac{\partial y}{\partial t} = -EI\frac{\partial^4 y}{\partial x^4} + As\frac{\partial^2 y}{\partial x^2} \qquad T = Exp\left(\frac{-c\,t}{2\rho A}\right)\cdot(A_1 sin\omega t + A_2 cos\omega t) \qquad \omega = \sqrt{\frac{1}{\rho}\left(\frac{n\pi}{L}\right)^2\left[\frac{EI}{A}\left(\frac{n\pi}{L}\right)^2 + s\right] - \left(\frac{c}{2\rho A}\right)^2}$$

Thus, the vibration frequency of the beam increases under stress s, making it a high-frequency mode. As high-frequency and normal mode NIED Hi-net high-sensitivity continuous waveform images, an example is a fore-seismic waveform map from the Mj6.4 11 km depth of the 2026.01.06.10h Shimane Prefecture Eastern Earthquake (observation points: Hakuta Shimane Prefecture, 01.05.16h, etc.). When analyzing the five P and S waves in the figure at frequency (0~45Hz), the maximum amplitude spectra in normal mode are concentrated in the low-frequency range, while in high-frequency mode, they are dispersed.

Since the rock strain energy is $\propto s^2/2E$, and the vibration energy is $\propto (A\omega)^2$, the seismic amplitude is $A^2 \propto (s/\omega)^2 \propto s$. If the stress/strain diagram of rock under high temperature and high pressure decreases just before fracture, as in usual rock and metallic materials, then after a foreshock of about Mj 4 , a high-frequency mode earthquake with a smaller amplitude of reduced stress occurs, it is increasing the likelihood of a major earthquake (main shock) occurring soon. This statistical analysis will likely be useful for investigating large earthquakes.

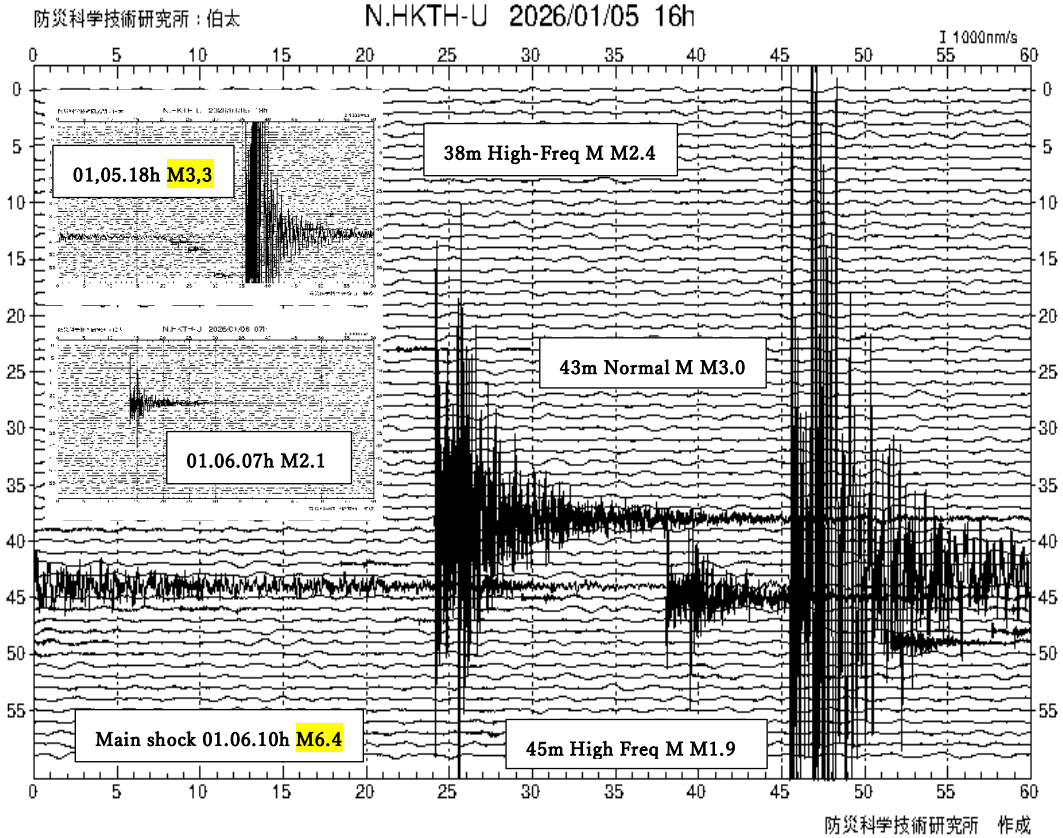

High-frequency/Normal mode :
Caused by the slippery/ non-slip collapse of the vulnerable asperity, conceptually involving viscous c. It also involves residual or dissipation of stress energy within the asperity influence range.

Data provided by NIED on the waveform images and JMA on the epicenter list to express gratitude.

The order of amplitude and frequency of vibration waveforms due to differences in stress and asperity breakdown modes acting on bedrock within the asperity influence range is as follows. Significant bedrock stress causes large amplitudes and high-frequency vibrations.

Ranking of Vibration Amplitude and Frequency in High-Sensitivity Seismic Waveform Diagrams

		Stress in bedrock		Note (Target: Mj3~Mj5 earthquakes)
		Near max. strength	Near breaking strength	
vibration amplitude	Hi-Frq. mode	②	④min. amp.*)	・The bedrock strain energy in the asperity influence range is residual/ dissipating in case of high-frequency /normal mode vibration.
	Normal mode	①max. amp.	③	
vibration frequency	Hi-Frq. mode	①max. frq.	③	
	Normal mode	②	④min. frq.	

*) Understanding this is important in case of predicting large earthquakes.

When the seismic waveform moves away from the epicenter, the amplitude decreases, the shaking duration lengthens, and the seismic waveform deteriorates as shown in the four diagrams below.

2026/01/05 18h obs p HKT①

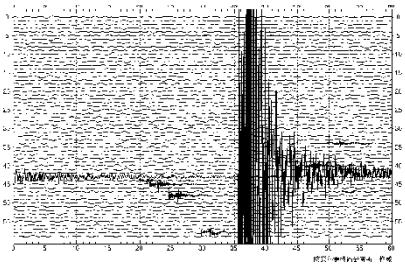

2026/01/05 18h obs p NIT②

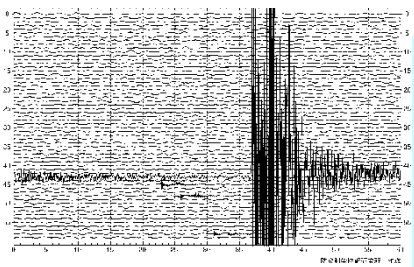

2026/01/05 18h obs p YSD③

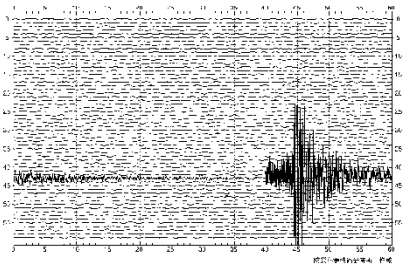

2026/01/05 18h obs p IWA④

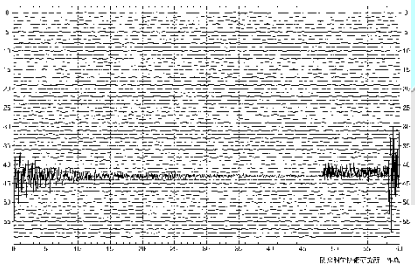

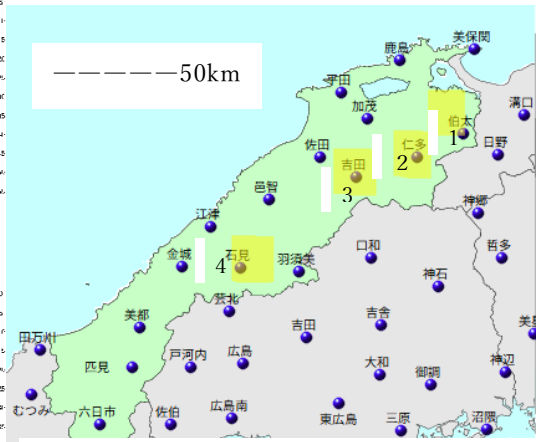

High Sensitivity Seismograph Network In Shimane Prf., Japan

Since continuous observation waveform data from 2007 onward can be viewed, it investigates the occurrence status of high-frequency vibrations immediately before 19 major earthquakes of Mj≧7. As a result, the assumption that it is increasing the likelihood of main shock occurring soon when high-frequency mode earthquake occurs after a foreshock of about Mj 4, to some extent, can be correct and is relatively reliable. The results of the hit ○ and miss × are shown in the following table (eleven ○ and eight ×).

Earthquakes of Mj7 or higher and examples of occurrence of high-frequency vibrations (hit ○ and miss×)

(hit ○ & miss×) Year/Date /Time of earthquakes	Epicenter and earthquake name, Magnitude	Observation Points	Foreshock date/time, (days until mainshock),M	High-freq. vib. date/ time before mainshock (days until mainshock), M
○ 2008/05/08 around 01h45m	Off Ibaragi Prf Mj7.0	Ibaragi Prf. Nakaminato	05/05 09 26 (3d) Mj5.1 05/07 18 59 (8h) Mj5.0	05/07 22h (4h) Mj－
× 2008/06/14 around 08h43m	Inland Southern Iwate Prf 2008 Mj7.2	Miyagi Prf. Kahoku	No prominent foreshock occurred	06/04 09h (10d) Mj3.0
× 2011/03/09 around 11h45m	Sanriku Off-Strait Mj7.3	Miyagi Prf. Kahoku	02/27 02 20 (10d) Mj4.7	03/06 21h (3d) epicenter unclear
× 2011/03/11 around 14h46m	Sanriku Off-Strait (**Great East Japan Earthquake 2011**) Mj9.0	Miyagi Prf. Kahoku	03/11 01 55 (13h) Mj5.4 03/11 06 50 (8h) Mj4.5	Impossible to distinguish due to the large number
× 2011/04/07 around 23h32m	Off Miyagi Prf Mj7.2	Miyagi Prf. Kahoku	04/05 13 25 (2d) Mj4.7 Many others	Numerous vibrations present, indistinguishable
○ 2011/04/11 around 17h16m	Hamadori, Fukushima Prf. Mj7.0	Fukushima Prf. Iwaki East	04/10 17 52 (1d) Mj3.8	04/10 22h (1d) M－
○ 2012/12/07 around 17h18m	Sanriku Off-Strait Mj7.3	Miyagi Prf. Kahoku	11/30 15 41 (7d) M4.6	12/0 7 06h (11h) M－
○ 2013/10/26 around 02h10m	Off Fukushima Prf Mj7.1	Fukushima Prf. Iwaki East	10/18 18 40 (7d) Mj4.2 10/22 10 18 (4d) Mj5.3	10/25 07h (1d) M－
○ 2014/07/12 around 04h22m	Off Fukushima Prf Mj7.0	Fukushima Prf. Iwaki East	07/05 23 59 (6d) Mj4.5	07/06 14h (6d) M－ 07/09 19h (3d) M－
× 2016/04/16 around 01h25m	2016 Kumamoto EQ. Mj7.3 2016/04/14 21h26m Mj6.5	Kumamoto Prf. Masiki	04/03 14 22 (12d) Mj2.2	04/06 16h (8d) Mj1.7
○ 2016/11/22 around 05h59m	Off Fukushima Prf Mj7.4	Fukushima Prf. Iwaki East	11/02 07 37 (20d) Mj4,9	11/19 22h (2d) Mj3.4
○ 2021/02/13 around 23h08m	Off Fukushima Prf Mj7.3	Fukushima Prf,Iwaki East	01/23 22 13 (21d) Mj4.5	01/31 15h (13d) Mj3.9
× 2022/03/16 around 23h34m	Off Fukushima Prf Mj7.4	Fukushima Prf.Iwaki East	02/26 08 32 (20d) Mj4.5	03/13 07h (4d) Mj3.8
○ 2024/01/01 around 16h10m	Noto Region, Ishikawa Prf. 2024 Noto Peninsula earthquake Mj7.6	Ishikawa Prf. Yanagida	12/21 05 11 (11d) Mj3.7 12/24 08 07 (8d) Mj3.7	12/27 22h (5d) Mj3.1
× 2024/08/08 around 16h43m	Hyuga Sea Mj7.1	Miyazaki Prf. Hyuga	07/30 01 25 (9d) Mj5.2	08/05 13h (3d) epicenter unclear
○ 2025/12/08 around 23h15m	Offshore to the east of Aomori Prf Mj7.6	Aomori Prf. Hachinohe	11/18 17 20 (20d) Mj4.7	11/30 08h (9d) Mj3.6
○ 2026/04/20 around 16h52m	Sanriku Off-Strait Mj7.7	Iwate Prf. Taro	04/08 15 28 (12d) Mj4.3	04/18 04h (3d) Mj3.2
○ 2026/06/25 around 07h30m	Off Iwate Prf Mj7.2	Iwate Prf. Kuji Kita	06/11 15 06 (14d) Mj3.7	06/17 21h (8d) Mj3.5 06/22 11h (3d) Mj2.8
× 2026/07/28 around 16h27m	2026 Kumamoto Earthquake Mj7.1	Kumamoto Prf. Toyono	No prominent foreshock occurred	07/17 20h (11d) Mj2.7